Mścisław ŚRUTEK, Tomasz ANDRYSIAK
University of Technology and Life Sciences, Bydgoszcz, Poland
mscislaw.srutek@utp.edu.pl, tomasz.andrysiak@utp.edu.pl

FLAME DETECTION BASED ON INFRARED IMAGES

Key words

Flame detection, infrared image, machining pursuit decomposition.

Summary

In this paper, we present a proposal of a method for the detection and localization of flames with the use of infrared images. In order to achieve this goal, an adaptive decomposition of an image has been used to search for adjusted elements of the Gabor dictionary. In our work, we used the Matching Pursuit algorithm [3]. Using decomposition coefficients of transformed infrared images, a coefficient of activity, characterizing the occurring thermal processes, has been defined. The method has been developed for the detection of flames and can find its application in intelligent surveillance and protection systems.

Introduction

Systems for fire detection whose function is most frequently based on automatic detectors are critically important for safety. These are usually different types of sensors that make use of chemical, ionizing, or thermal phenomena, which makes it possible to detect flames or smoke. More advanced solutions make use of multi-sensor technologies, enabling one to detect fire threats more efficiently. A drawback of these detectors is their inability to

pinpoint the place of fire formation, thereby, its (immediate) point neutralization.

In the recent years, we have witnessed a development of research concerning the application of video camera images for the detection of flames and smoke, thanks to their ability to make an analysis of motion and colour [6, 10, 19]. Research has been conducted on a method for smoke detection based on wavelet transform and vector machines [9], where video from industrial CCD cameras were used. To reduce amount of false alarms in smoke detection, an accumulative motion model based on the integral image by fast estimating the motion orientation of smoke was devised [20].

Most fire detection in colour video sequences methods make use of various visual characteristics, including colour, motion, and the geometrical contour of flame. In [15] the presented method, the temporal accumulation of time derivative images to extract the best candidate fire region in video image is used. There were many researches on detecting fire in road and rail tunnels. Neural network was used for vehicle fire detection in tunnels [16], but the results depended on the distance of the vehicle and the CCD colour camera. Good results are provided by an algorithm that uses YcBcR colour space to separate the luminance from the chrominance, which works more effectively than colour spaces such as RGB [5].

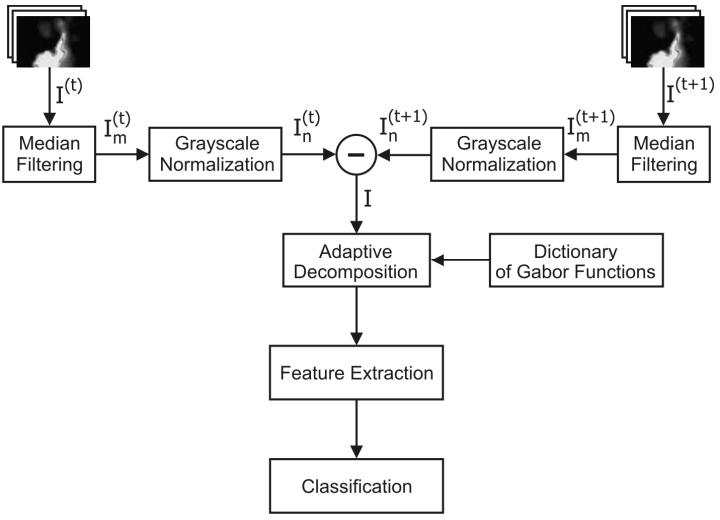

Fig. 1. General scheme of our solution

According to our approach, an algorithm of adaptive decomposition has been used in order to detect flames by means of infrared images. In the initial stages of transformation, the operations of median filtration and the

normalization of transformed the images' grey levels are performed. Next, the differential image is calculated (Fig. 1) which is the result of subtraction of successive images selected from a video sequence. For such an image, adaptive decomposition operations are performed for selected and adjusted elements of the Gabor dictionary. Calculated decomposition coefficient residues and atoms applied from the dictionary define the search for the coefficient of thermal activity. The calculated coefficient is compared, in the process of classification, with the assigned threshold value, in order to make a decision on the existence of flames or their absence.

1. Median Filtering and Image Grayscale Normalization

The best-known order-statistics filter is the *median filter,* which replaces the value of a pixel by the median of the grey levels in the neighbourhood of that pixel.

$$I_m(x,y) = median_{(s,t)\in W} I(s,t) \tag{1}$$

The original value of the pixel is included in the computation of the median. In our case, we use window $W = 3 \times 3$ elements. As a result of median filtration, we receive image I_m.

After filtering the image, we normalize all its regions to a certain mean and variance. Normalization is performed to remove the effects of sensor noise and grey level deformation. Moreover, the extraction of salient points, performed later in our method, depends on the illumination variance in the image. Therefore, in order to achieve illumination and contrast invariance, we normalize the image.

Let $I_m(x, y)$ denote the grey value at the pixel (x, y), E and V be the estimated mean and illumination variance in the image I_m, respectively, and $I_n(x, y)$ stand for the normalized graylevel value at the pixel (x, y).

For all the pixels in the image I_m, the normalization process is defined as follows:

$$I_n(x,y) = \begin{cases} E_0 + \sqrt{\frac{V_0(I_m(x,y)-E)^2}{V}} & if\ I_m(x,y) > P, \\ E_0 - \sqrt{\frac{V_0(I_m(x,y)-E)^2}{V}} & otherwise \end{cases} \tag{2}$$

where E_0 and V_0 are the desired mean and variance values, respectively, and E and V are the computed mean and variance in the given image, described by

$$E = \frac{1}{MN}\sum_{x=0}^{M-1}\sum_{y=0}^{N-1} I_m(x,y) \tag{3}$$

$$V = \frac{1}{MN}\sum_{x=0}^{M-1}\sum_{y=0}^{N-1}(I_m(x,y) - E)^2 \tag{4}$$

respectively. In our case, E_0 = 100, V_0 = 100 and P = 128. As a result of the operation of luminance level normalization, we obtain image I_n.

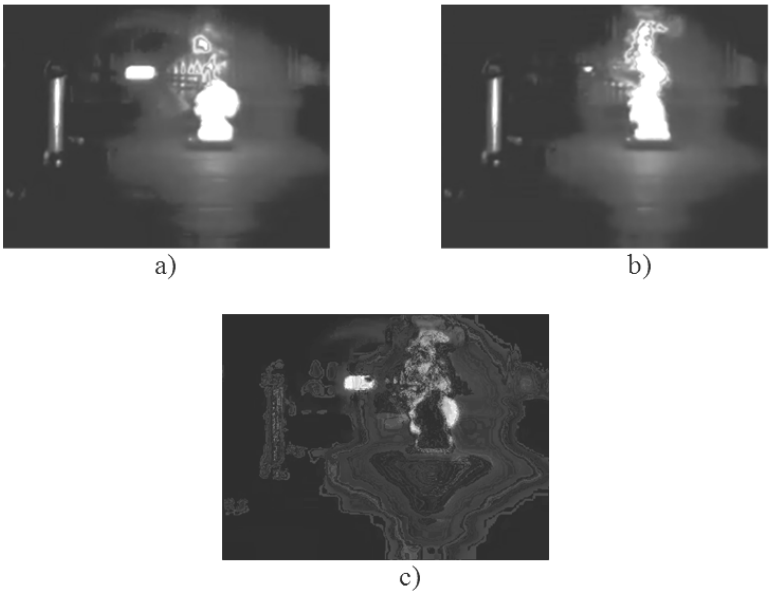

Fig. 2. Normalized infrared images: a) image $I_n^{(t)}$ in time t, b) image $I_n^{(t+1)}$ in time $t+1$, c) differential image $I = I_n^{(t+1)} - I_n^{(t)}$

2. Flame Detection System based on Adaptive Decomposition of Images

Decomposition of a differential image I, leading to its adaptive representation through a choice of a set of atoms g_γ from D dictionary, is reduced to the problem of their best match with the analysed image I, that is, the minimization of approximation error δ [7].

$$\delta = \left\| I - \sum_{i=1}^{M-1} \alpha_i g_{\gamma_i} \right| \tag{5}$$

Optimal representation can be defined as a subset of the dictionary elements whose linear combination accounts for the highest signal energy percentage among all equally numerous subsets. Choosing this representation is difficult in terms of computing; thus, in practice, we are satisfied with an iteration adaptive solution known as MP [4, 18] algorithm. The result of this algorithm is a projection of the signal structural elements on functions chosen from the dictionary, called atoms [3].

2.1. Matching Pursuit Overview

In order to perform decomposition of image *I*, we determine linear development for atoms of set g_γ chosen from dictionary *D,* so that they will be best matched with structural elements of the analysed image *I*.

In each step of the MP algorithm, the image *I* will be further decomposed by orthogonal projections on the elements of the dictionary D. Then, in n-th step of decomposition, we obtain the following:

$$R^n I = R^{n-1} I - \langle R^{n-1} I, g_{\gamma_{n-1}} \rangle g_{\gamma_{n-1}} \tag{6}$$

where <*, *> stands for scalar product and $R^n I$ is a residue being the effect of decomposition *I* in the direction g_γ. For a residue of zero order, there occurs an obvious dependence $R^n I = I$.

The atom g_γ is chosen based on the following:

$$g_{\gamma_n} = arg \max_{g_{\gamma_i} \epsilon G} \left| \langle R^{n-1} I, g_{\gamma_i} \rangle \right| \tag{7}$$

where *G* is a set of dictionary *D* indexes.

Then, it is possible to calculate decomposition coefficient:

$$\alpha_n = \langle R^{n-1} I, g_{\gamma_n} \rangle \tag{8}$$

For atom g_γ chosen by means of Dependence (7), residue is minimized in the next step *n* of algorithm MP. Due to the orthogonality of vectors g_γ and $R^n I$, there occurs the following relation:

$$\|R^{n-1} I\|^2 = \left| \langle R^{n-1} I, g_{\gamma_{n-1}} \rangle \right|^2 + \|R^n I\|^2 \tag{9}$$

Continuing the decomposition process to *N*-th level, we obtain

$$R^N I = I - \sum_{n=0}^{N-1} \langle R^n I, g_{\gamma_n} \rangle g_{\gamma_n} \tag{10}$$

Similar to (9), we can write

$$\|I\| = \sum_{n=0}^{N-1} \left|\langle R^n I, g_{\gamma_n}\rangle\right|^2 + \|R^n I\|^2 \tag{11}$$

Thus, we obtain the equation of energy conservation [3, 14].

The number of N iterations, in which decomposition of residues is performed, depends on the accuracy required for the reconstruction of image I and is given by Dependence (12), being at the same time a stop criterion of the MP algorithm.

$$\|R^N I\|^2 \leq \beta \|I\|^2 \tag{12}$$

where parameter $\beta \in (0, 1)$.

The rate of the residue norm decrease depends on a correlation between the successive residues of images and atoms chosen from the dictionary. If the image is a sum of component s with high energy, being atoms of the dictionary, then the image correlation coefficients and its residues are significant. Then, their norm decreases rapidly, as components with high energy are the image structural elements well correlated with the atoms chosen from the dictionary [8].

2.2. Dictionary of Gabor Functions

An exact representation of the analysed image in a dictionary is larger than the base introduces redundancy. The desired conciseness can be achieved accepting some imperfections of the image reconstruction, but with the use of possibly small number of functions [17].

In the described solution, we propose a waveform from the time frequency dictionary which can be expressed as translation (u), dilation (ϑ) and modulation (φ) of a window function $g(x) \in L^2(R)$

$$g(x) = \frac{1}{\sqrt{s}} e^{-\pi x^2} \tag{13}$$

Then, set $Z = R^+ \times R^2$ is defined, $\gamma_k \in Z$ atom indexes $\gamma_k = \{u_k, \vartheta_k, \varphi_k\}$, where parameter u is responsible for scaling, ϑ is a shift, and φ modelling frequency [11, 14]:

$$g_{\gamma_k}(x) = \frac{K_{\gamma_k}}{\sqrt{u_k}} g\left(\frac{x\vartheta_k}{u_k}\right) \cos(x\vartheta + \varphi_k) \tag{14}$$

where $\vartheta_k \neq 0$, phase $\varphi_k \in (0,2\pi)$, and constant K_{γ_k} is matched so that $\left\|g_{\gamma_k}\right\| = 1$.

Using properties of two-dimensional decompositions of the Gabor function, it can be written as

$$g_{\gamma_n}(x,y) = g_{y_k}(x) \times g_{\gamma_l}(y) \tag{15}$$

where $\gamma_k = \{u_k, \vartheta_k, \varphi_k\}$ and $\gamma_l = \{u_l, \vartheta_l, \varphi_l\}, respectively$.

In Table 1 there are presented values of parameters (u, ϑ, φ) used in the Gabor dictionary atom ***creation process based on Dependence (15).

Table 1. Parameters for the Gabor atoms [1]

n	u	ϑ	φ
1	2	0	0
2	3	0	0
3	4	0	0
4	5	0	0
5	6	0	0
6	8	0	0
7	10	0	0
8	11	0	0
9	1	1	π / 2
10	5	1	π / 2
11	11	1	π / 2
12	10	3	0
13	8	2	0
14	4	2	0
15	4	2	π / 4
16	6	4	π / 4

In Fig. 3, there is an image of the Gabor dictionary modelled by means of parameters defined in Table 1.

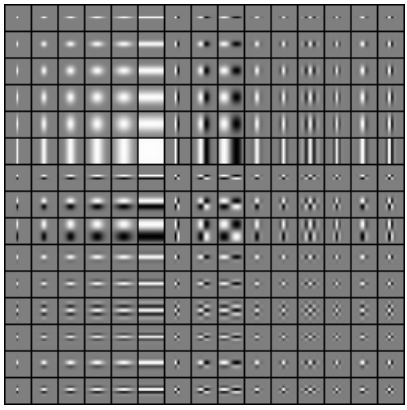

Fig. 3. Gabor dictionary

2.3. Flame Feature Extraction Based on Adaptive Decomposition

The matching pursuit algorithm produces three important elements of information:

- The set of decomposition coefficients $\alpha = \{\alpha_0, \alpha_1, \ldots, \alpha_{n-1}\}$,
- The set of residues $RI = \{R^0 I, R^1 I, \ldots, R^{n-1} I\}$, and
- The list of dictionary elements chosen to approximate of *I(x, y)*, represented as $g_\gamma = \{g_{\gamma_0}, g_{\gamma_1}, \ldots, g_{\gamma_{n-1}}\}$.

This three factors, α, *RI* and g_γ, completely define the image *I(x, y)*. Their energies can be written according to the following equation:

$$E = \|\alpha\| + \|RI\| + \|g_\gamma\| \tag{16}$$

The value of E parameter univocally characterizes the context content of the analysed differential images *I(x, y)*.

3. Experimental Results

A record of inflammable substance combustion was performed in a Combustion Laboratory of Polon-Alfa in cooperation with the Institute of Optoelectronics at the Military University of Technology in Warsaw [2]. The combustion process was performed in appropriately normalized measurement conditions.

The choice of recorded wavelengths was made based on earlier measurements of radiation spectrums of inflammable substances with the use of an infrared spectroradiometer. An increase in energy emission for the infrared radiation waves with length 4–5 μm was observed for different substances.

Table 2. Experimental results of tested video sequences

Id	E	Decision
1	2.46e+6	Yes
2	1.72e+6	Yes
3	0.93e+2	No
4	9.61e+5	Yes
5	1.12e+6	Yes
6	8.77e+5	Yes
7	1.12e+3	No
8	2.08e+5	Yes
9	8.71e+5	Yes
10	1.72e+3	No

To record flames, infrared video camera FLIR GF 320, operating in the wavelength of 3–5 μm, was used, which recorded all the images with resolution 320 x 240 pixels. On the basis of an analysis of literature, [10, 11, 12, 13], and the authors' own observations, the frequency of recorded images was accepted to be 3 Hz. Images of combusted petrol 95 and isopropyl alcohol were analysed. Interferences in the form of a quartz and soda lamps were added to the studied images. In the successive stage, a noise in the form of a large fan was added. Its blades periodically covered the recorded sources of heat.

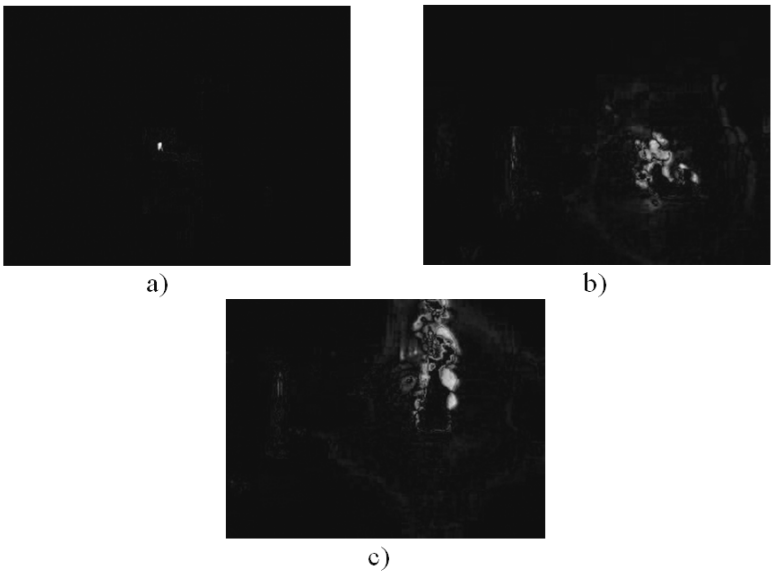

Fig. 4. Examples of images from tested video sequences: a) image from Id = 3, b) image from Id = 8, c) image from Id = 5

In order to verify the proposed methodology, we used a data set of 50 video sequences – 25 with flames, and 25 without flames. Each sequence consists of 300 images/frames (100 sec.). Sample differential images are presented in Fig 4. The sample results are given in Table 2 (values of energy E, threshold, and decision (yes for detected flames, no otherwise)). The threshold value for flames detection was set to P = 1.0e+4. Detection Rate was 92% (the system correctly detected 23 out of 25 flame sequences), while False Positives ratio was 0% (no false alarms in 25 sequences without flames). For the tested images, we noticed a trend of increasing energy E for increased thermal dynamics. We also performed some experiments in order to localize detected flames by using positions of Gabor atoms used in MP algorithm. However, the obtained results were satisfactory only for atoms characterized by high value of luminance mean.

4. Conclusions and Future Work

In the article, a method for the detection of flames with the use of an analysis of infrared images has been discussed. Successive stages of infrared variance images transformations involving their normalization, adaptation, and adaptive decomposition based on Marching Pursuit robust algorithm that searches for and matches elements of a given dictionary to the analysed image structure have been presented. As a result of experiments, it was found that the presented method is characterized by a high interference resistance and allows the localization of the source of heat.

In order to accomplish the goals of this study, methods allowing the system to search for the atoms in the context of the analysed images have been studied.

Further works will aim at increasing the fire detection coefficient with simultaneous maintenance of high interference resistance.

References

1. Banham M.R., Brailean J.C.: A selective update approach to matching pursuits video coding, IEEE Transactions on Curcuits and Systems Video Technology, vol. 7, no. 1, pp. 119–129 (1997).
2. Bareła J., Kastek M., Firmanty K., Polakowski H.: Measurements of the radiation spectra of flammable substances using infrared Spectroradiometer (in Polish), Materiały konferencyjne TTP (2009).
3. Bergeaud F., Mallat S.: Matching pursuit of images, In Proc. IEEE International Conference on Image Processing ICIP'95, vol. 1, pp. 53–56 (1995).
4. Bruckstein A.M., Donoho D.L., Elad M.: From sparse solutions of systems of equations to sparse modeling of signals and images, SIAM Review, vol. 51, no. 1, pp. 34–81 (2009).
5. Celik T., Demirel H.: Fire Detection in video sequences using a generic color model, Fire Safety Journal, vol. 44, pp. 147–158 (2009).
6. Chunyu, Y., Jun, F., Jinjun, W., Yongming, Z.: Video Fire Smoke Detection Using Motion and Colour Features, Fire Technology, vol. 46, pp. 651–663 (2010).
7. Davis G., Mallat S., Avellaneda M.: Adaptive greedy approximations, Journal of Constructive Approximation, vol. 13, pp. 57–98 (1997).
8. Elad M.: Sparse and Redundant Representations: From Theory to Applications in Signal and Image Processing, Springer (2010).
9. Gubbi J., Marusic S., Palaniswami M.: Smoke detection In video Rusing wavelet and suport vector machines, Fire Safety Journal, vol. 44, pp. 1110––1115 (2009).

10. Han D., Lee B.: Flame and smoke detection method for early real-time detection of a tunnel fire, Fire Safety Journal, vol. 44, pp. 951–961 (2009).
11. Janssen A., Gabor representation of generalized functions, Journal of the Mathematical. Analysis. and Applications, vol. 83, no. 2, pp. 377–394 (1981).
12. Ko B.C., Cheong K.H., Nam J.Y.: Early fire detection algorithm based on irregular patterns of flames and hierarchical Bayesian Networks, Fire Safety Journal, vol. 45, pp. 262–270 (2010).
13. Ko B.C., Cheong K.H., Nam J.Y.: Fire detection based on vision sensor and support vector machines, Fire Safety Journal, vol. 44, pp. 322–329 (2009).
14. Mallat S., Zhang Z.: Matching pursuits with time-frequency dictionaries, IEEE Transactions on Signal Processing, vol. 41, no. 12, pp. 3397–3415 (1993).
15. Marbach G., Loepfe M., Brupdacher T.: An image processing for fire detection in video images, Fire Safety Journal, vol. 41, pp. 285–289 (2006).
16. Ono T., et al.: Application of neural network to analyses of CCD colour TV-camera image for the detection of car fire in expressway tunnels, Fire Safety Journal, vol. 41, s. 279–284 (2006).
17. Rubinstein R., Bruckstein M., Elad M.: Dictionaris for Sparse Representation Modeling, Proceedings of the IEEE, vol. 98, pp. 1045–1057 (2010).
18. Tropp J.A.: Greed is good: Algorithmic results for sparse approximation, ICES Report 03-04, The University of Texas at Austin (2003).
19. Yuan F.: An integrated fire detection and suppression system based on widely available video surveillance, Machine Vision and Applications, vol. 21, pp. 941–948 (2010).
20. Yuan F.: A fast accumulative motion orientation model based on integral image for video smoke detection, Pattern Recognition Letters, vol. 29, pp. 925–932 (2008).

Wykrywanie płomieni z wykorzystaniem obrazowania w podczerwieni

Słowa kluczowe

Wykrywanie płomieni, obrazy termowizyjne, dekompozycja Maching Pursuit.

Streszczenie

W pracy zaproponowano metodę wykrywania i lokalizacji płomieni na podstawie analizy sekwencji zdjęć wykonanych techniką podczerwieni. Aby

osiągnąć ten cel, przetwarzane obrazy poddano operacji poprawy jakości, a następnie odejmowano je od siebie w celu wyznaczenia obrazów różnicowych. Tak otrzymane obrazy poddawano operacji adaptacyjnej dekompozycji z zastosowaniem odpowiednio modelowanych funkcji Gabora w oparciu o algorytm Matching Pursuit. Bazując na algorytmie dekompozycji, zdefiniowano współczynnik aktywności termicznej, charakteryzujący wykryte procesy na obrazach wykonanych w podczerwieni. Opracowana metoda pozwala na wykrywanie i lokalizacje płomieni ze współczynnikiem wykrywalności True Positive równym 92%. Opisywane rozwiązanie może znaleźć zastosowanie w inteligentnych systemach monitoringu i ochrony przeciwpożarowej.